



HAL
open science

EMI Frequency Model of a Low Power SMPS in Discontinuous Conduction Mode

Yandry Jacome, Jugoo Ansley, Mohamed Toure, Schanen Jean-Luc

► **To cite this version:**

Yandry Jacome, Jugoo Ansley, Mohamed Toure, Schanen Jean-Luc. EMI Frequency Model of a Low Power SMPS in Discontinuous Conduction Mode. ECCE USA 2024, Oct 2024, Phoenix, United States. hal-04780658

HAL Id: hal-04780658

<https://hal.science/hal-04780658v1>

Submitted on 13 Nov 2024

HAL is a multi-disciplinary open access archive for the deposit and dissemination of scientific research documents, whether they are published or not. The documents may come from teaching and research institutions in France or abroad, or from public or private research centers.

L'archive ouverte pluridisciplinaire **HAL**, est destinée au dépôt et à la diffusion de documents scientifiques de niveau recherche, publiés ou non, émanant des établissements d'enseignement et de recherche français ou étrangers, des laboratoires publics ou privés.

EMI Frequency Model of a Low Power SMPS in Discontinuous Conduction Mode

JACOME Yandry

Somfy
74300 Cluses, France
yandry.jacome@somfy.com

JUGOO Ansley

Univ. Grenoble Alpes, CNRS
Grenoble INP, G2Elab
38000 Grenoble, France
ansley.jugoo@grenoble-inp.fr

TOURE Mohamed

Somfy
74300 Cluses, France
mohamed.toure@somfy.com

SCHANEN Jean-Luc, *Fellow IEEE*

Univ. Grenoble Alpes, CNRS
Grenoble INP, G2Elab
38000 Grenoble, France
jean-luc.schanen@grenoble-inp.fr

Abstract— This paper describes an EMC model in the frequency domain suitable for a DC-DC converter operating in Discontinuous Conduction Mode. In comparison to Continuous Conduction Mode, an additional phase appears, with voltage oscillations, which must be considered. The frequency model is presented and its implementation using LT Spice is described. It is validated in comparison with time domain simulations and measurements, for the application of a roller shutter. Finally, a fine tuning of the EMC model parameters is also presented for the industrial implementation of the converter.

Keywords—EMC, Modeling, Power Electronics, Identification

I. INTRODUCTION

With advances in wide-bandgap semiconductors, switching frequency and switching speed have increased dramatically, bringing ElectroMagnetic Compatibility (EMC) issues back to the fore, as they were in the 90s. Many efforts are being made to reduce the size of switch-mode power supplies (SMPS), whose results can be completely negated when EMC standards have to be met... Sometimes in a whole system, the main origin of ElectroMagnetic Interferences (EMI) is not straightforward. The example of roller shutters used in this paper is an interesting case study of a situation where the efforts made by EMC engineers on the power system design (a DC brushless drive) to meet the EN-55014 EMC standard were destroyed when considering the 1 W power supply used for auxiliaries and communication features ! This paper shows a quick and easy-to-implement EMI model allowing the EMC investigation of a full system. It is classically based on equivalent sources in the frequency domain, as already presented in many papers [1-3]. Time domain simulation exhibits too many convergence issues and is hard to be used in a complete design workflow. Therefore, the current and voltage discontinuities of the SMPS are replaced by equivalent sources and the resulting circuit can then be solved directly in the frequency domain. However, especially in low power, the DC-DC converters are not operated in Continuous Conduction Mode (CCM), but often enter in Discontinuous Conduction Mode (DCM) due to low average current. This impacts the EMI generation, with potentially modified propagation paths, higher peak currents and additional oscillations which must be considered in the EMC model. The goal of this paper is to show how to introduce this operating mode in an EMC frequency model. First, the conventional frequency modeling approach will be reminded for a buck converter in CCM. The implementation of the model in

LT Spice using Laplace transform controlled sources will be shown, and the results compared with time domain simulations (Section II). Section III will then show how to modify the disturbance sources to match with the DCM operating conditions. The model will be implemented with LT Spice in the same way as CCM, and compared to both Time Domain simulation and measurement, based on a simple evaluation board. Section IV will show a realization of two cascaded DC-DC converters implemented on a PCB, using some integrated devices. In this situation, it is not obvious to determine all values of the parameters which should be used in the EMC model. Therefore, an optimization algorithm will be used to determine the main parameters of the model, to match the EMI measurement results.

II. EMC FREQUENCY MODEL IN CCM

A. EMC Model

Investigating EMI using time domain simulation is feasible for simple topologies, using detailed High Frequency models for each component of the converter (active, passive and interconnects). However, multiplying the number of converters leads to several well-known issues as convergence problems, simulation time and size of the output files. Therefore, many authors have proposed to replace the switching devices by equivalent sources [1-3], reproducing the voltage and current discontinuities. The obtained circuit is then solved directly in the frequency domain. Fig. 1 shows the illustration of this modeling method in the simple case of a Buck Converter operating in Continuous Conduction Mode. The current discontinuity at converter's input is reproduced with a current source corresponding to the MOSFET's current, whereas the voltage quick change at floating point is considered with a voltage source corresponding to MOSFET's V_{DS} voltage.

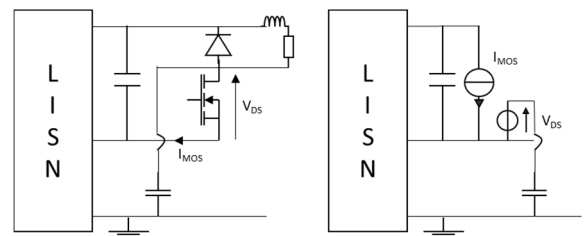


Fig. 1. Frequency Model of a buck converter connected to a Line Impedance Stabilization Network (LISN). The switches are replaced by equivalent sources corresponding to MOSFETs current and voltage.

This equivalent circuit includes the load behavior in the current source I_{MOS} (as the impact of the output ripple current, ...) and V_{DS} can reproduce all fluctuations of the input DC bus, as well as potential ripples at MOSFET turn off. Usually, in the frequency range of interest, between the switching frequency up to few MHz, the DC bus can be considered constant, and the output current modeled with a triangular waveform. Therefore, the time domain representation of I_{MOS} and V_{DS} are the simplified ones, displayed in Fig. 2. The corresponding Laplace expressions of these waveforms are given by Eq. (1) and (2). To be noticed that the coefficient $2.fsw$ is added in these Laplace expressions to account for the periodicity of the signals (switching frequency $fsw = 1/Tsw$). The duty cycle d is defined in Fig. 2.

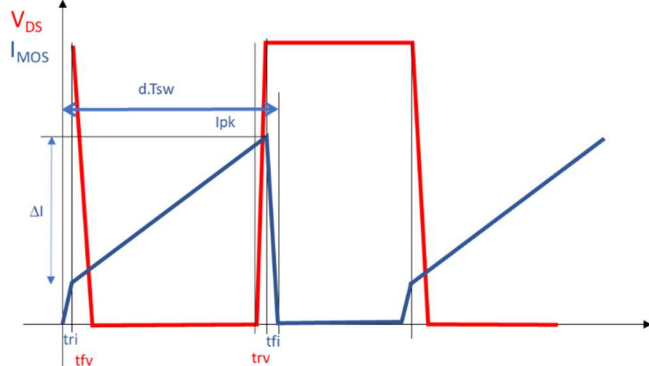


Fig. 2. Time domain representation of $V_{DS}(t)$ and $I_{MOS}(t)$ used in the Laplace transform expressions (CCM).

$$I_{MOS}(s) = 2 \cdot fsw \cdot \left[\frac{(I_{pk} - \Delta I)}{tri \cdot s^2} \cdot (1 - \exp(-s \cdot tri)) + \exp(-s \cdot tri) \cdot \frac{\Delta I}{(d \cdot Tsw - tri - tfi) \cdot s^2} \cdot (1 - \exp(-s \cdot (d \cdot Tsw - tfi - tri))) - \exp(-s \cdot (d \cdot Tsw - tfi)) \cdot \frac{I_{pk}}{tfi \cdot s^2} \cdot (1 - \exp(-s \cdot tfi)) \right] \quad (1)$$

$$V_{DS}(s) = 2 \cdot fsw \cdot \left[\exp(-s \cdot tri) \cdot \frac{-V_{dc}}{tfv \cdot s^2} \cdot (1 - \exp(-s \cdot tfv)) + \exp(-s \cdot (d \cdot Tsw - tfi - trv)) \cdot \frac{V_{dc}}{trv \cdot s^2} \cdot (1 - \exp(-s \cdot trv)) \right] \quad (2)$$

B. Model implementation with LT Spice

Another representation of the frequency model of Fig. 2 can be proposed in Fig. 3. This other representation is identical. Indeed, using a superposition theorem, it is obvious that the current source is still in parallel with input capacitance, and the floating point is still excited by V_{DS} . In this paper this equivalent model will be used, since it allows a bit more genericity for more complex topologies as illustrated in [4] in the case of a multilevel boost converter.

The model can be directly implemented and solved in LT Spice (Fig. 4) using Voltage Controlled Voltage Source (E) and Voltage Controlled Current sources (G), controlled by Laplace expressions defined in LT Spice, corresponding to the waveforms of MOSFET drain current (1) and drain to source voltage (2).

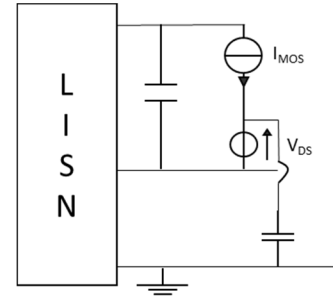


Fig. 3. Another representation of the Frequency Model of Fig. 2.

This is a very convenient solution, since the use of Laplace expression allows quickly describing the switching waveforms. Care must be taken to the time origin, which defines the phase shift between V_{DS} and I_{MOS} , but it is much easier than expressing the Fourier series.

Fig. 4 shows the two representations of the buck converter, one used in the time domain simulation, and the other being the equivalent EMC frequency model. The parameters of the sources (rise and fall times tri , tfv , tfi , trv , peak and ripple current I_{pk} , ΔI , as well as duty cycle d and switching period Tsw) have been adjusted between the two models. The values of all elements of the circuit, including the ones used for the LISN (Line Impedance Stabilization Network) are provided in Table I. It should be noted that the values are taken from the example which will be detailed in section IV, and correspond to a situation with very low common mode stray capacitance. This is a specific situation, which does not affect the general applicability of the proposed model, which has been validated in many previous works.

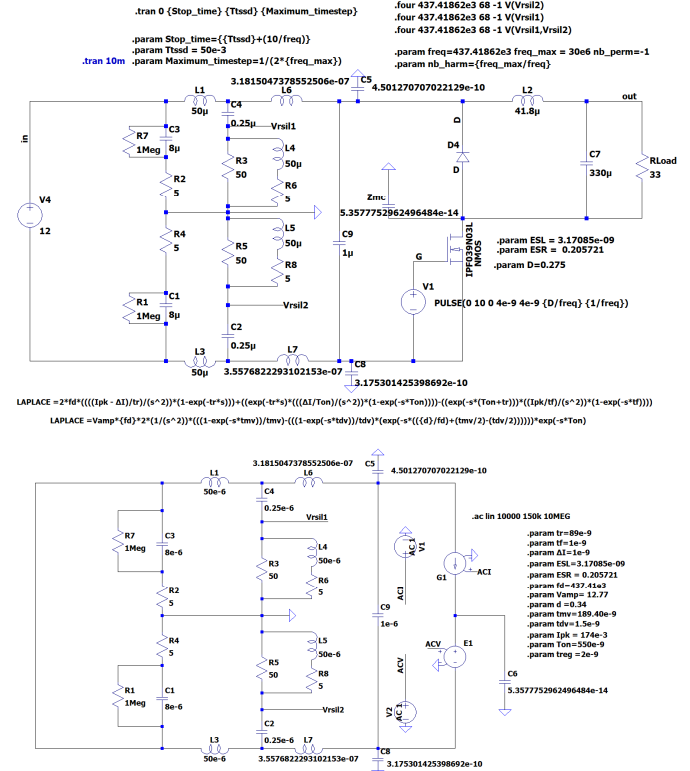


Fig. 4. A buck converter operating in CCM. Top – time domain model. Bottom – frequency model. The values of elements are provided in Table I.

TABLE I. BUCK CONVERTER MODEL PARAMETERS

System	Component values (time domain)		
	Designation	Value	Unit
LISN	C1, C3	8	μF
	L1, L3	50	μH
	R2, R4	5	Ω
	C2, C4	0.25	μF
	R3, R5	50	Ω
	L4, L5	50	μH
	R6, R8	5	Ω
	Cable	L6	318 (not coupled)
L7		356 (not coupled)	nH
Converter	Input Capacitor	1	μF
	ESL	3.17	nH
	ESR	0.2	Ω
	C5	450	pF
	C8	317	pF
	Zmc	0.05	pF
	L2	41.8	μH
	C7	330	μF
	Fsw	437.4	kHz
	d	0.275	--

C. Frequency model results

Fig. 5 shows the good agreement of the peaks of the FFT of the LISN voltages (phase and neutral) after a time domain simulation, in comparison with the envelope obtained by the Frequency Model using Laplace expressions. The simulation time is almost instantaneous using this Frequency Model (0.4 s vs 30 mn). The results of Fig. 5 are in line with the existing literature, and show the outstanding performance of the Frequency Model for quick EMC investigations. Obviously, replacing the semiconductors by equivalent sources is an approximation, which becomes no longer valid beyond few MHz, but this is often sufficient for EMI filter design.

Unfortunately, this kind of model has not been reported for converters operating in Discontinuous Conduction Mode (DCM). This is the objective of the following section.

III. EMC FREQUENCY MODEL IN DCM

A. EMC Model

The main change in DCM is that three different phases are to be considered: one with the MOSFET in the on state and Diode off, one with the MOSFET off and Diode on, and the last one with both devices off (“Idle” phase).

This modifies both current and voltage waveforms, and may affect the validity of the equivalent circuit. The DCM operation has not been extensively addressed in the literature, and even though, no model were given [5-8].

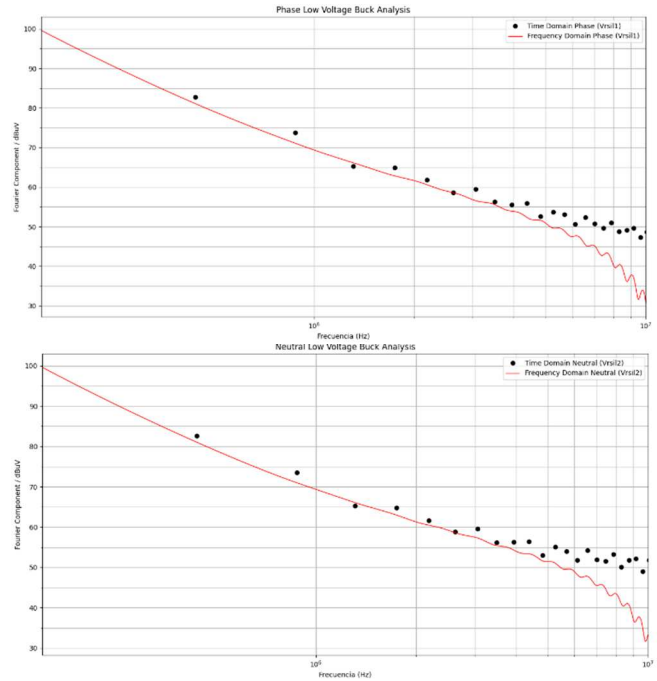


Fig. 5. Frequency Model results for LISN Voltage in LT Spice for a Buck Converter in CCM (envelope) – Comparison with time domain simulation (FFT). The peaks are exactly matching the Laplace envelope till few MHz.

The oscillations on voltage and current appearing in the additional “Idle” phase (Fig. 6) are due to the resonance between the output inductor and device’s capacitance C_{oss} & C_{diode} . This phenomenon results in a medium frequency oscillation (around 900kHz in the example of Fig. 6) which generates a peak in the frequency domain, which may violate the standard. Also the current shape is modified, since it is now a triangular current starting from zero, and not an almost trapezoidal waveform for an “infinite” output inductor. The large peak seen on the current waveform at MOSFET turn-on results from the sudden discharge of the devices capacitances, which state during the “idle” phase was uncontrolled. This peak shown in the simulation of Fig. 6 actually occurs experimentally, as it will be shown in section IV.

The idea of the EMC model for DCM is to keep the same topology as the equivalent circuit used for CCM, and modify the sources only. This seems to be quite a fair assumption, since the additional voltage and current oscillations will be reproduced by the sources, and generate the corresponding EMI noise. To start simple, only the oscillation of the voltage source has been implemented, since the amplitude of the current oscillation is very small in our example. Also the current peak at turn on has not been included in the model, since its prediction is not easy. The consequence of this peak, which acts as a Dirac delta function, will correspond in the frequency domain to add a constant value. This neglected phenomenon can be considered later.

The modified Laplace expressions of the sources I_{mos} and V_{ds} are given by Eq (3) and (4). To keep it simple, the attenuation of the sinewave has not been taken into account. All parameters describing the waveforms (rise and fall times t_{fv} , t_{rv} , t_{fi} , peak current I_{pk} , duty cycle d , duration of diode conduction β , t_{sw} , and oscillation parameters ω , A) are illustrated in Fig. 7.

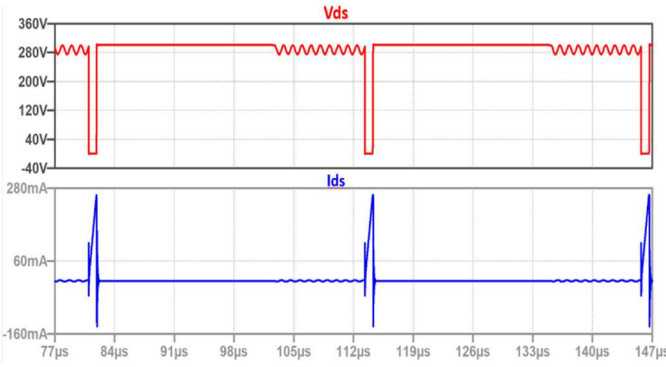


Fig. 6. Simulated waveforms of a Buck Converter in DCM. Top: MOSFET Voltage – Bottom: MOSFET Current

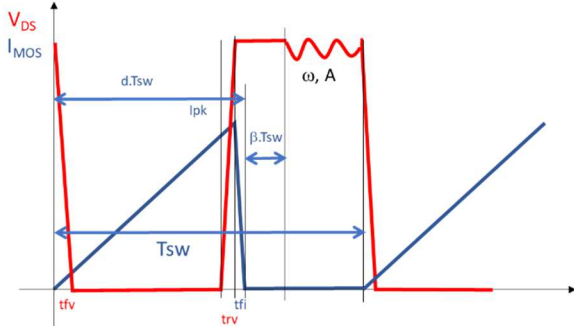


Fig. 7. Time domain representation of $V_{DS}(t)$ and $I_{MOS}(t)$ used in the Laplace transform expressions (DCM).

$$I_{MOS}(s) = 2 \cdot f_{sw} \cdot \left[\frac{I_{pk}}{(d \cdot T_{sw} - t_{fi}) \cdot s^2} \cdot (1 - \exp(-s \cdot (d \cdot T_{sw} - t_{fi}))) - \exp(-s \cdot (d \cdot T_{sw} - t_{fi})) \cdot \frac{I_{pk}}{t_{fi} \cdot s^2} \cdot (1 - \exp(-s \cdot t_{fi})) \right] \quad (3)$$

$$V_{DS}(s) = 2 \cdot f_{sw} \cdot \left[\frac{-V_{dc}}{t_{fv} \cdot s^2} \cdot (1 - \exp(-s \cdot t_{fv})) + \exp(-s \cdot (d \cdot T_{sw} - t_{fi} - t_{rv})) \cdot \frac{V_{dc}}{t_{rv} \cdot s^2} \cdot (1 - \exp(-s \cdot t_{rv})) - \exp(-s \cdot (d + \beta) \cdot T_{sw}) \cdot \frac{A \cdot \omega}{\omega^2 + s^2} \right] \quad (4)$$

B. EMC Model Validation

To validate the model in DCM, a time domain simulation and the frequency model implementation in LT Spice have been compared, as for CCM. The Buck converter used converts 300 V DC into 12V DC, with a very low power, less than 1W. Since the Frequency Model in DCM was never presented up to now, an experimental validation was also necessary. A simple evaluation board was used to build this buck converter operating in DCM, in order to allow some internal measurements. The circuit schematic for the time domain is given in Fig. 8, the main parameters of this converter being summarized in Table II. They have been determined thanks to a characterization of the evaluation board elements. An input filter is included in this board (C5-L8). The wires between the LISN and the converter were simply modeled with two uncoupled inductors (L3, L7). They were quite distant from the ground plane so that the stray capacitive effects were neglected.

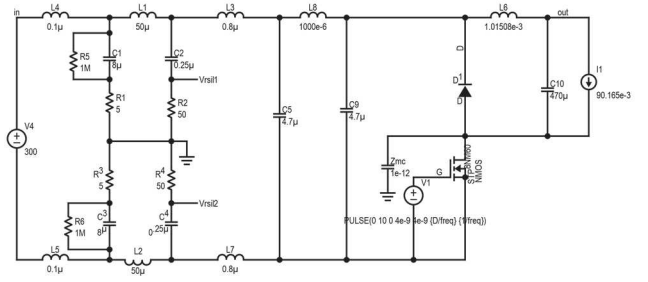


Fig. 8. LT Spice time domain simulation schematics. The frequency model is identical to the one presented in Fig. 4-bottom, only the expressions of the sources have been modified, according to Eq (3) and (4).

TABLE II. BUCK CONVERTER MODEL PARAMETERS FOR DCM

Component values			
System	Designation	Value	Unit
Cable	L3	800 (not coupled)	nH
	L7	800 (not coupled)	nH
Filter	C5	4.7	μ F
	ESL	5	nH
	ESR	1	m Ω
	L8	1	mH
	EPR	11.5	k Ω
	EPC	7.8	pF
Converter	Input Capacitor C9	4.7	μ F
	ESL	5	nH
	ESR	1	m Ω
	Zmc	1	pF
	L6 (assumed ideal)	1	mH
	C10	470	μ F
	ESR	1	m Ω
	ESL	5	nH
Fsw	30	kHz	
d	0.0288	--	

The evaluation board and the corresponding experimental waveforms are provided in Fig. 9, as well as the EMC measurement setup. As already discussed, the oscillations on the MOSFET's voltage can be clearly seen, as well as the peak current at MOSFET turn-on, which is however lower than in the simulation.

Fig. 10 shows that both Frequency Model and time domain simulation are matching quite well together and also with the measurement, until almost 10 MHz. The peak at ~ 900 kHz induced by the voltage oscillation in the "Idle" phase is clearly visible, even if it is localized at lower frequency in the experimental results, due to a bad estimation of the model parameters (semiconductors, stray elements, output inductor considered ideal...). The values of A and ω of the frequency model were: $A = 300$ and $\omega = 2\pi \cdot 926.6$ kHz.

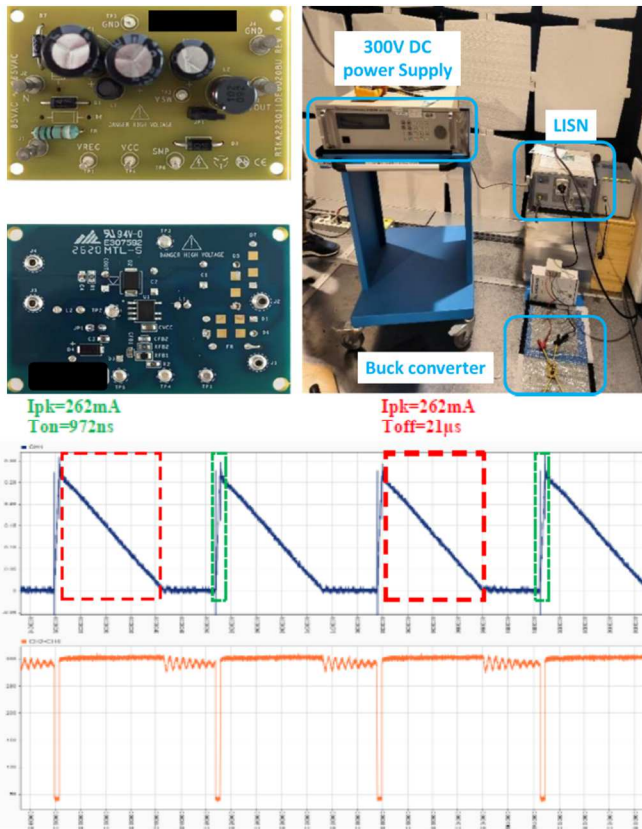


Fig. 9. Top: evaluation board used for Buck Converter operating in DCM. and EMC setup - Bottom: experimental waveforms (switch voltage and inductor current).

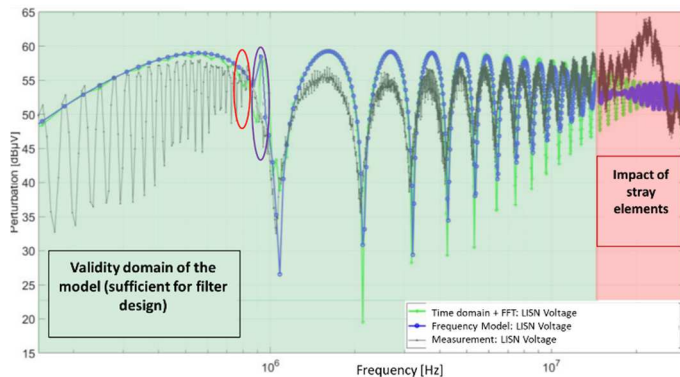


Fig. 10. Comparison of the LISN phase voltage obtained by the Frequency Model, a time domain simulation and measurement.

This section has shown that a Frequency Model of a Buck converter operating in DCM can be obtained simply by modifying the sources used in the conventional Frequency Model of a Buck in CCM. Only the voltage ringing has been considered, others factors as peak current at MOSFET turn on could also be added, to further improve the model. The results have been validated in comparison with a time domain simulation, and with experiment, obtained on a simple evaluation board. The next section will apply both Frequency Models in CCM and DCM to a full industrial application, implemented in a very dense PCB.

IV. APPLICATION: POWER SUPPLY OF A ROLLING SHUTTER

A. System Description

Fig. 11 shows the schematic view of the low power Switched Mode Power Supply (SMPS) used in a roller shutter system. It is composed of two different parts: a High Voltage Buck Converter (HVBC) converts 300V into 12V to supply a DC brushless motor and also a Low Voltage Buck Converter (LVBC), to feed all low power communication electronics @3.3V. The HVBC operates in DCM at 30.9 kHz, with very low duty cycle ($d = 0.0095$), whereas the LVBC switches at 437.4 kHz with $d = 0.275$.

The majority of the time, the drive is not in use, and the HVBC just delivers the 12V to feed the LVDC. Therefore, it operates at 1 W, and in DCM. The LVBC delivers around 0.6 W and operates in CCM. However, the global converter has to meet the EMC standard, even at low power ! Therefore, there is a strong need to investigate the EMC performances of these converters. The EMC Frequency Model is here a very powerful tool.

Both HVBC and LVBC are implemented in a very highly integrated PCB (Fig. 11). The board has been realized in two versions: one with the HVBC components only, and one with only the LVBC devices soldered. This allows the construction and validation of the two EMC models separately.

B. Model Parameter Estimation

At first, the bare PCB without any devices was characterized with an impedance analyzer, to obtain an estimate of the Common Mode Capacitances. The task was tricky since the distance to the ground plane was not fixed, no shielding layer being integrated in the PCB. An insulated foam was inserted between the PCB and the copper plane used in the EMC characterization to impose a constant distance.

The second issue is that in such integrated circuit, using integrated devices, no waveform measurement is possible, and not all devices were available in the LT Spice library. Therefore, it was decided to set up a dedicated process to evaluate the stray elements of the model, in order to validate the modeling approach. This process, illustrated in Fig. 12, uses an optimization strategy to fit the EMC measurement results as best as possible. Of course, this is useless in a real world where the EMC model should be used in a predictive way, but in this paper, the goal is to show that the modeling method is valid. Therefore, it is valuable to try to match simulation and experimental results as much as possible, to show that the model has captured all the hardware behavior.

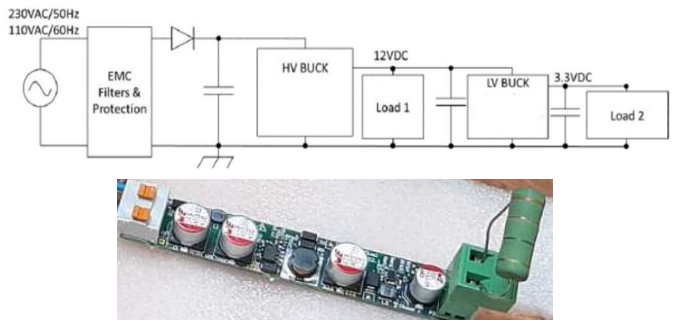


Fig. 11. Top: overview of the low power converter composed of a HVBC cascaded with a LVBC. Bottom: realization with a highly integrated PCBs.

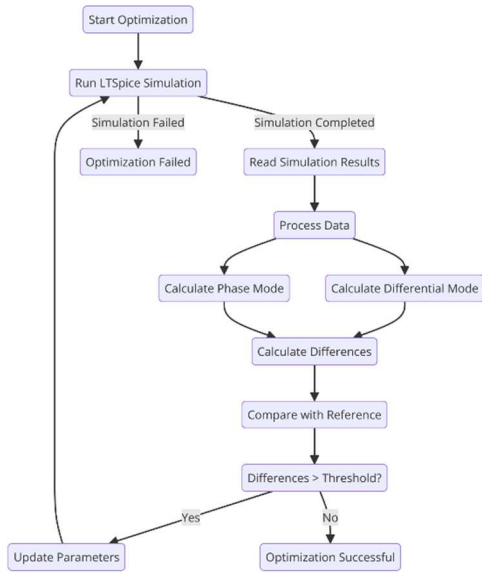


Fig. 12. Optimization process to identify all stray elements. The EMC frequency models are included into an optimization loop to identify the model parameters, thanks to a comparison between measured and simulated Common Mode and Differential Mode noise.



Fig. 13. EMC measurement setup using EMScope device.

The measurement setup used to record Common Mode (CM) and Differential Mode (DM) noise is based on an EMScope device [9] allowing mode separation (Fig.13). The measured DM and CM noises are used in the optimization process, with the variable input parameters of the EMC models to be determined. To reduce the number of parameters, it has been decided to change the interconnects, PCB and devices parameters only. The disturbance sources were kept constant. Since no oscillation were seen in the HVBC operating in DCM, it was decided to not use the model with the sinewave in eq (4), and just keep a trapezoidal waveform.

It is worth noting that this optimization approach is only achievable by using the Frequency Model, which are very quick to solve: it would not have been possible to conduct this approach with a time domain simulation due to simulation time and convergence issue.

The following subsections will provide the EMC spectra obtained after optimization, and compare the Frequency Model outcomes to the time domain simulation and measurement results.

C. Results of the Low Voltage Buck Converter (CCM)

Fig. 14 shows the results of the Frequency Model after stray elements adjustment by the optimization algorithm, in the CM/DM basis, in comparison with both a time domain simulation and the measurement used for model identification. The CM noise is very low (around 30 dB μ V), and very hard to distinguish from the background noise (around 20 dB μ V). Therefore, only the fundamental at 437.4 kHz can be seen in the measurement. However, the time domain simulation with the set of identified parameters matches quite well with the Frequency Model. The values of all elements are the ones which were provided in Table I, section II-B.

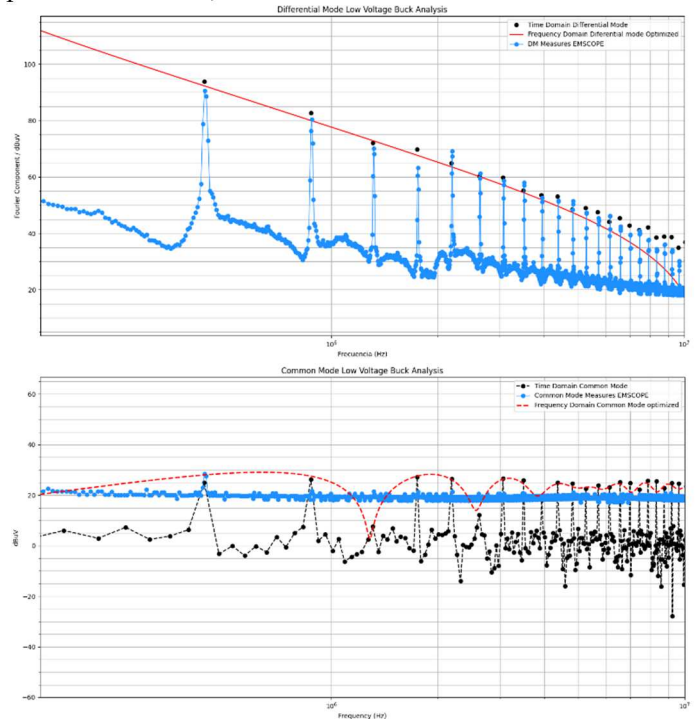


Fig. 14. LVBC LISN voltage results after optimized parameters. Comparison between Frequency Model, time domain simulation and measurement. Top: DM noise, bottom CM noise.

D. results of the High Voltage Buck Converter (DCM)

The values of the stray elements obtained after adjustment by the optimization algorithm. are displayed in Table III. The simulation schematic for the time domain is shown in Fig. 15 (the frequency model is derived from the method of Fig. 3).

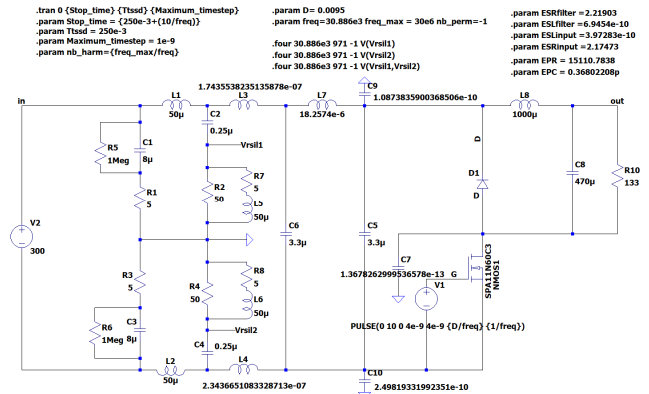


Fig. 15. HVBC schematics with optimized stray elements (values in Table III).

TABLE III. HVBC MODEL PARAMETERS (DCM)

System	Component values		
	Designation	Value	Unit
Cable	L3	174 (not coupled)	nH
	L4	234 (not coupled)	nH
Filter	C6	3.3	μ F
	ESL	0.7	nH
	ESR	2.2	Ω
	L7	18.26	μ H
	EPC	0.37	pF
	EPR	15111	Ω
	Converter	Input Capacitor C5	3.3
	ESL	3.2	nH
	ESR	206	m Ω
	C9	109	pF
	C10	250	pF
	Zmc (C7)	0.14	pF
	L8	1	mH
	EPC	4.7	pF
	EPR	170	k Ω
	C8	470	μ F
	ESL	5	nH
	ESR	1	m Ω
	Fsw	30.9	kHz
	d	0.0095	--

The value of ESR of the filter capacitor C6 is quite high, but it was mandatory to match better the measurement results in the medium frequency range. This phenomena will have to be investigated further in future work, by characterizing the device alone (maybe the component was damaged). Another explanation could also be the too simple source representation, without the peak in the current at MOSFET turn-on.

Fig. 16 shows the results of the Frequency Model after stray elements adjustment, in comparison with time domain simulation and the measurement used for model identification. The CM noise is higher than in the case of LVBC, and is reproduced quite well. The DM noise from the model matches also well the measurement, until the background noise (20 dB μ V) is reached. These good results validate the modeling approach proposed in this paper.

V. CONCLUSION

This paper has shown a unified approach to provide an equivalent frequency model for a Buck Converter operating either in CCM or DCM. The model for CCM was already well known from the literature, and this paper showed a very convenient way to introduce it in a simple LT Spice circuit, using controlled sources driven by Laplace expressions.

The operation in DCM exhibits different current and voltage waveforms in the switches, and it was demonstrated that introducing these new shapes in the conventional model allows a quite good estimate of the EMI disturbances. Not all phenomena have been implemented in the sources, only the voltage oscillation during the “Idle” phase. Future work may include the current peak at MOSFET turn on, as well as oscillation in the current source, in order to further refine the model.

This modeling approach was validated with an experimental converter built using an evaluation board, which stray elements were quite well known. It also allowed the measurement of the devices’ voltages and currents. Therefore, the Frequency Model parameters were obtained quite easily.

Eventually, the modeling approach was applied to a full system composed of two cascaded Buck Converters, one High Voltage operating in DCM, and one Low Voltage in CCM. The high level of integration of this system of converters did not allow the evaluation of the model parameters. Therefore, an optimization process was built in order to tune the main parameters of the Frequency Models, so as to match the EMC measurements.

The adjusted models matched quite well the measurement, what proves that the main phenomena have been taken into account.

Further work might investigate the impact of the sources, which have been kept constant in the identification process. Also a method to obtain the model parameters in a predictive way should be developed, especially for DCM (in particular the amplitude and frequency of the oscillation).

Finally, the association of the two cascaded converters should be studied.

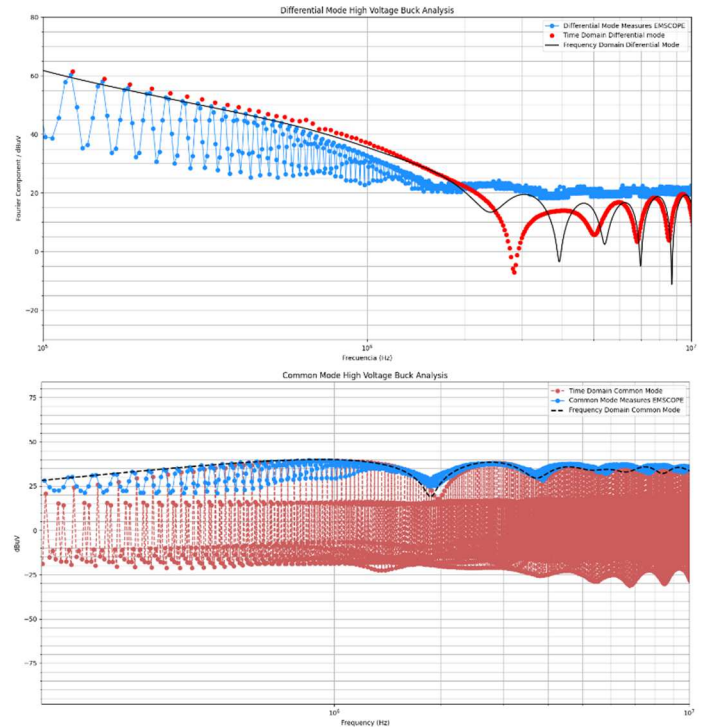


Fig. 16. HVBC LISN voltage results after optimized parameters. Comparison between Frequency Model, time domain simulation and measurement. Top: DM noise, bottom CM noise.

REFERENCES

- [1] B. Touré, J-L. Schanen, L. Gerbaud, T. Meynard and J. -P. Carayon, "EMC modelling of drives for aircraft applications: Modelling process and optimisation of EMI filters," Proceedings of the 2011 14th European Conference on Power Electronics and Applications, Birmingham, UK, 2011, pp. 1-10.
- [2] S. Vienot, A. Videt, N. Idir, L. Kone, S. Weiss and F. Lafon, "Frequency-domain simulation of power electronic systems based on multi-topology equivalent sources modelling method," 2020 22nd European Conference on Power Electronics and Applications (EPE'20 ECCE Europe), Lyon, France, 2020, doi: 10.23919/EPE20ECCEurope43536.2020.9215867. keywords:
- [3] B. Nassireddine, B. Abdelber, C. Nawel, D. Abdelkader and B. Soufyane, "Conducted EMI Prediction in DC/DC Converter Using Frequency Domain Approach," 2018 International Conference on Electrical Sciences and Technologies in Maghreb (CISTEM), Algiers, Algeria, 2018, pp. 1-6, doi: 10.1109/CISTEM.2018.8613398.
- [4] M.Tadbiri, J.L.Schanen, H.Imaneini, L.Alves, "Optimization of EMI Filters of Multi-Level Flying Capacitor Boost Converter", IEEE transactions on Industry Applications, DOI: 10.1109/TIA.2024.3425796, <https://ieeexplore.ieee.org/document/10592799> (early access)
- [5] Q. Ji, X. Ruan, L. Xie and Z. Ye, "Conducted EMI Spectra of Average-Current-Controlled Boost PFC Converters Operating in Both CCM and DCM," in IEEE Transactions on Industrial Electronics, vol. 62, no. 4, pp. 2184-2194, April 2015, doi: 10.1109/TIE.2014.2361483.
- [6] J. Wang and J. Xu, "Peak Current Mode Bifrequency Control Technique for Switching DC–DC Converters in DCM With Fast Transient Response and Low EMI," in IEEE Transactions on Power Electronics, vol. 27, no. 4, pp. 1876-1884, April 2012, doi: 10.1109/TPEL.2011.2170591.
- [7] P. Zumel, O. García, J. A. Oliver and J. A. Cobos, "Differential-Mode EMI Reduction in a Multiphase DCM Flyback Converter," in IEEE Transactions on Power Electronics, vol. 24, no. 8, pp. 2013-2020, Aug. 2009, doi: 10.1109/TPEL.2009.2019648.
- [8] J. C. Crebier, P. Barbosa, F. Canales, F. C. Lee and J. P. Ferrieux, "Frequency domain analysis and evaluation of differential mode input current for three-phase DCM boost rectifiers with different control strategies," 2000 IEEE 31st Annual Power Electronics Specialists Conference. Conference Proceedings (Cat. No.00CH37018), Galway, Ireland, 2000, pp. 482-487 vol.1, doi: 10.1109/PESC.2000.878908.
- [9] https://emzer.com/?gad_source=1&gclid=EAlaIqObChMlrdO1uPC9hwMVBjdoCR3COQqEEAAYASAAEgLJrvD_BwE [online, accessed July 24th, 2024]